RESEARCH ARTICLE

High-frequency (50 Hz) electroacupuncture ameliorates cognitive impairment in rats with amyloid beta 1–42-induced Alzheimer's disease

Chao-Chao Yu[1,#], Ying Wang[1,#], Feng Shen[2], Li-Hong Kong[2,*], Ya-Wen Wang[2], Hua Zhou[2], Lei Tang[3]

1 Hubei University of Chinese Medicine, Wuhan, Hubei Province, China

2 Department of Acupuncture and Moxibustion, College of Acupuncture and Orthopedics, Hubei University of Chinese Medicine, Wuhan, Hubei Province, China

3 Department of Rehabilitation, Wuhan Central Hospital Affiliated to Tongji Medical College, Huazhong University of Science and Technology, Wuhan, Hubei Province, China

Funding: *This study was supported by the National Natural Science Foundation of China, No. 81373741; a grant from the Chinese Medicine and Integrated Medicine Research Projects funded by the Health and Family Planning Commission of Hubei Province of China, No. 24; a grant from the Hubei Provincial Collaborative Innovation Center of Preventive Treatment by Acupuncture and Moxibustion of China in 2014, No. 8.*

Graphical Abstract

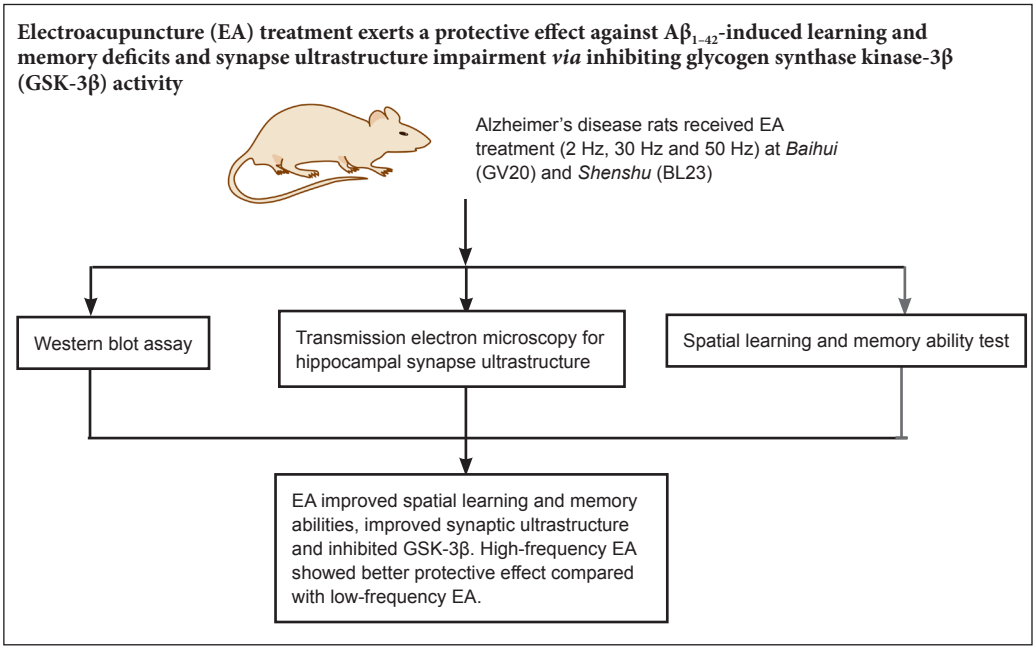

Correspondence to:
Li-Hong Kong,
xiyu1618@sina.com.

#These authors contributed equally to this study.

orcid:
0000-0002-4287-0536
(Li-Hong Kong)

doi: *10.4103/1673-5374.238620*

Accepted: *2018-07-14*

Abstract

Acupuncture has been shown to ameliorate cognitive impairment of Alzheimer's disease. Acupoints and stimulation frequency influence the therapeutic effect of electroacupuncture. Rat models of Alzheimer's disease were established by injecting amyloid beta 1–42 ($A\beta_{1-42}$) into the bilateral lateral ventricles. Electroacupuncture at 2, 30, and 50 Hz was carried out at *Baihui* (GV20; 15° obliquely to a depth of 2 mm) and *Shenshu* (BL23; perpendicularly to 4–6 mm depth), once a day for 20 minutes (each), for 15 days, taking a break every 7 days. The Morris water maze test was conducted to assess the learning and memory. The expression levels of glycogen synthase kinase-3β (GSK-3β), pSer9-GSK-3β, pTyr216-GSK-3β, amyloid precursor protein and $A\beta_{1-40}$ in the hippocampus were determined by western blot assay. Results demonstrated that electroacupuncture treatment at different frequencies markedly improved learning and memory ability, increased synaptic curvatures, decreased the width of synaptic clefts, thickened postsynaptic densities, and downregulated the expression of GSK-3β, amyloid precursor protein, and $A\beta_{1-40}$. pSer9-GSK-3β expression markedly decreased, while pTyr216-GSK-3β expression increased. High-frequency (50 Hz) electroacupuncture was more effective than low (2 Hz) or medium-frequency (30 Hz) electroacupuncture. In conclusion, electroacupuncture treatment exerts a protective effect against $A\beta_{1-42}$-induced learning and memory deficits and synapse-ultrastructure impairment *via* inhibition of GSK-3β activity. Moreover, high-frequency electroacupuncture was the most effective therapy.

Key Words: *nerve regeneration; electroacupuncture; different frequencies; Alzheimer's disease; cognitive impairment; hippocampus; glycogen synthase kinase-3β; synaptic curvatures; width of synaptic cleft; postsynaptic density; Baihui (GV20); Shenshu (BL23); neural regeneration*

Introduction

Alzheimer's disease (AD) is the most prevalent cause of dementia and is characterized by progressive memory deficits and cognitive decline. The pathological features associated with cognitive dysfunction are neurofibrillary tangles and senile plaques, combined with neuronal loss primarily in the hippocampus and other important cortical and subcortical brain regions (Hane et al., 2017). Hyperphosphorylated tau protein molecules bundle to form intracellular neurofibrillary tangles (Kocahan and Dogan, 2017) and abnormal amyloid precursor protein (APP) metabolism results in extracellular deposition of amyloid beta (Aβ) (Selkoe and Hardy, 2016). Approximately 40 million people worldwide are estimated to be affected by dementia, among which most are people over 60 years old. This figure is expected to double every 20 years until at least 2050, making it one of the biggest threats to health in older people and one of the biggest overall healthcare issues (Prince et al., 2013). Although the situation is severe, no effective therapy is yet capable of alleviating symptoms or slowing down disease progression (Folch et al., 2016). Searching for effective AD therapies has become a key goal in public health.

The synapse is the structural basis for connections between neurons. A recent study has shown that AD can be viewed as a failure in structure and function (Selkoe, 2002). Glycogen synthase kinase-3β (GSK-3β) is a serine/threonine protein kinase that is linked to the cleavage of abnormal APP (Muresan and Muresan, 2005) and is involved in neuronal apoptosis (Beurel and Jope, 2006) and inducing tau hyperphosphorylation (Brugg and Matus, 1991). GSK-3β displays high activity under resting/basal conditions. Its constitutive activity is reduced upon N-terminal serine-9 phosphorylation and stimulated by tyrosine-216 phosphorylation (Llorens-Martín et al., 2014). As the key regulator in Wnt signaling, changes in GSK-3β activity are associated with synaptic plasticity, which has been established as a cellular model for learning and memory (Liang and Chuang, 2007). Along the same lines, overexpression of GSK-3β results in spatial learning deficits (Hernández et al., 2002). Inhibition of GSK-3β can inhibit Aβ-plaque deposition, increase the number of synapses and postsynaptic density thickness, and rescue the reduction of spine density in the hippocampal CA1 area of APP/PS1 mice (Zhang et al., 2016a). All these indicate that regulating the expression and activity of GSK-3β may be a promising approach for treating AD (Balaraman et al., 2006).

Exploring both safe and effective therapy aimed at inhibiting GSK-3β as a treatment for AD has drawn growing attention. However, a phase-II trial using the GSK-3β inhibitor tideglusib to treat AD demonstrated that administering it to patients with mild-to-moderate AD over 26 weeks was acceptable in terms of safety, but did not produce any clinical benefit (Lovestone et al., 2015).

Some researchers have proposed that exploring Chinese medicine as an alternative therapy and source for discovering novel drugs could lead to potential treatments for AD (Law et al., 2017). A systematic review has also concluded that Chinese acupuncture was safe and effective for treating AD in terms of improving cognitive function (Zhou et al., 2015). Both acupoint selection and frequency of electroacupuncture (EA) stimulation play a significant role in EA-induced effects (Zhu et al., 2015). Kidney deficiency and *Du* meridian occlusion as a consequence of *qi* stagnation and blood stasis are regarded as the major cause of senile dementia based on Chinese medicine theory. Thus, the acupoints *Shenshu* (BL23) and *Baihui* (GV20) have usually been chosen to nourish kidney-essence and modify the Governor vessel. Clinical trials have also shown that acupuncture at GV20 and BL23 can improve the cognitive ability and activities of daily living in patients with AD (Peng and Dong, 2009; Zhu et al., 2010). Accumulating evidence has shown that the effects of EA on the central nervous system depend on the frequency of stimulation, indicating that EA frequency may be related to the therapeutic effects of EA (Cheng et al., 2012; Wang et al., 2012; Lin et al., 2013; Kimura et al., 2015). However, the optimal EA-stimulation frequency for AD treatment has yet to be standardized. Thus, exploring and identifying the best EA frequency for treating AD is important.

In our previous studies, high-frequency EA alleviated $A\beta_{1-42}$-induced cognitive impairments by reducing synapse loss in the hippocampus (Wang et al., 2016), upregulating the expression of synaptic markers, such as postsynaptic density-95 and synaptophysin (Zhang et al., 2016b), enhancing hippocampal synaptic transmission (Li et al., 2016), and attenuating tau hyperphosphorylation (Gao et al., 2017). However, the effect of EA on other key characteristics of AD, such as synapse ultrastructure and APP, remains uncertain. Aβ species are responsible for initiating a pathogenic cascade, thereby leading to synaptic dysfunction, neuronal loss and cognitive deficits (Selkoe and Hardy, 2016). According to the prevailing amyloid-cascade hypothesis, abnormal APP cleavage processing and Aβ deposits are believed to induce tau hyperphosphorylation and neurofibrillary tangle formation, leading to synaptic dysfunction (Selkoe, 2002). Overproduction of the Aβ peptide, which is found in both familial forms of AD and late-onset AD, supports its central role in AD pathogenesis and correcting Aβ dyshomeostasis is now a compelling therapeutic strategy (Selkoe and Hardy, 2016). Thus, the present study observed the effects of different EA frequencies on hippocampal synapse ultrastructure and cognitive function in rat models of AD that were established by intracerebroventricular injection of $A\beta_{1-42}$ (O'Hare et al., 1999). We also measured the expression and activity levels of GSK-3β, APP, and $A\beta_{1-40}$, which are mechanistically important for AD synapse pathology.

Materials and Methods

Animals and model establishment

Fifty-six adult male Wistar rats aged 4–5 months and weighing 310 ± 20 g were provided by the Hubei Provincial Laboratory Animal Research Center of China (license number: SCXK (E) 2008-0005) and were randomly assigned to seven groups (n = 8 per group): control, sham operation, model

(AD), sham EA (AD + sham EA), 2-Hz EA (AD + 2-Hz EA), 30-Hz EA (AD + 30-Hz EA), and 50-Hz EA (AD + 50-Hz EA). The rats were housed (n = 4 per cage) at 20 ± 2°C with a relative humidity of 50% ± 10% under a 12-hour light/dark cycle (lights on at 8:00 a.m.) and were given free access to food and water. Ethical approval for this study was provided by the Animal Ethics Committee of the Hubei University of Chinese Medicine, China.

Rats in the model, sham EA, 2-Hz EA, 30-Hz EA, and 50-Hz EA groups were intraperitoneally anesthetized with of 10% chloral hydrate (3.5 mL/kg; Sinopharm Chemical Reagent Co., Ltd., Wuhan, China). Afterward, 5 μL of normal saline (sham operation group) or aggregated $A\beta_{1-42}$ (2.5 μg/μL; Sigma, St. Louis, MO, USA; model, sham EA, 2-Hz EA, 30-Hz EA, 50-Hz EA groups) was injected over 5 minutes using a Hamilton microsyringe into the bilateral lateral ventricles (−3.2 mm posterior to the bregma, ± 2.5 mm lateral to the midline, and 3.5 mm below the dura, according to a stereotaxic atlas of the rat brain; Paxinos and Franklin, 2004). The needle was maintained in place for an additional 3 minutes to allow diffusion into the surrounding tissue before being slowly retracted. $A\beta_{1-42}$ was first dissolved in distilled water and then diluted in phosphate buffer saline (PBS) at a concentration of 2.5 μg/μL and incubated for 5 days at 37°C to ensure aggregation before the injection.

EA treatment

Starting on day 7 after $A\beta_{1-42}$ injection, sham EA was administered to sham EA group; 2-Hz EA, 30-Hz EA, and 50-Hz EA were administered to 2-Hz EA, 30-Hz EA, and 50-Hz EA groups at GV20 and alternating unilateral BL23 once daily for 15 days with one rest day every 7 days. GV20 was located at the center of the parietal bone, and the needle was inserted into the epicranial aponeurosis. BL23 was located adjacent to the second lumbar vertebra (Guo and Kong, 2016). Rats receiving EA treatment were not anesthetized, but were wrapped in a conscious state and prone position with tailored, soft cloth materials. EA was delivered using stainless steel needles (15 mm in length and 0.3 mm in diameter; Suzhou Medical Apparatus Co., Ltd., Suzhou, China) and an EA apparatus (HANS-100A, Beijing Huayun Ante Science and Technology Co., Ltd., Beijing, China). At GV20, the needle was inserted 15° obliquely to a depth of 2 mm. At BL23, the needle was inserted perpendicularly to a 4–6-mm depth. Stimulation was applied to the pair of acupuncture points (GV20 and alternating unilateral BL23) in a continuous wave at 2 Hz, 30 Hz, or 50 Hz (depending on the experimental group) for 20 minutes each day. The intensity (1 mA) was adjusted to induce light muscle contractions. In the sham EA group, only the surfaces of GV20 and BL23 were stimulated, but the needles were inserted without current. Rats in the control, sham operation, and model groups were wrapped in the same way but received no other interventions.

Morris water maze test

Spatial memory function was evaluated using the Morris water-maze test (Bromley-Brits et al., 2011) on the 1st day after EA treatment. The apparatus (Chengdu Taimeng Technology Co., Ltd., Chengdu, China) consisted of a large circular pool (120 cm in diameter, 50 cm in height) and a MT-200 Morris water maze video-tracking system (Chengdu Taimeng Technology Co., Ltd., Chengdu, China). Data were recorded with the Watermaze 2.0 software (Chengdu Taimeng Technology Co., Ltd.). The pool was filled with opaque water (24 ± 1°C) to a depth of 40 cm with white milk and divided into four equal quadrants. The circular platform (10 cm in diameter) was placed at the midpoint of the target quadrant and submerged approximately 1.5 cm below the surface of the water. The rats were trained for 4 days on standard place-navigation trials. Each rat was placed into a quadrant facing the wall of the pool on four occasions (every time in different quadrants). The rats were given no more than 120 seconds to find the hidden platform in each trial and the time was recorded as the escape latency. When the rats failed to find the platform within this period, researchers would assist it onto the platform and keep the rat sitting on the platform for 10 seconds. The rats rested for 30 seconds between trials. For the spatial probe trial (conducted 1 day after the place navigation test), the platform was removed from the pool. This test was performed in the same way as the place navigation test. The rats were given 120 seconds to swim in the pool. The time spent in the target quadrant (the quadrant where the hidden platform was during training trials) and the number of times the rat crossed the location where the platform was during training were recorded.

Observation of transmission electron microscopy

At the end of EA treatment, half of the rats in each group were intraperitoneally anesthetized by 10% chloral hydrate immediately after the Morris water-maze test and transcardially perfused with 4% paraformaldehyde/2% glutaraldehyde in 0.1 M phosphate, pH 7.4. Their brains were separated by usual dissection methods and 1 mm^3 brain tissue blocks were immediately cut from the hippocampal CA1 area, and postfixed in 4% paraformaldehyde for 2 hours. After fixation, the samples were washed with PBS, postfixed with 1% osmium tetroxide for 1.5 hours, again washed in PBS, dehydrated in an acetone series, and then embedded in epoxy resin. Tissue blocks were then cut into 1-μm-thick thin sections. After uranyl acetate/lead citrate double staining, synapse ultrastructure was observed using a transmission electron microscope (7700; Hitachi, Tokyo, Japan). Synapse images were randomly obtained. According to the method utilized by Itarat and Jones (1993), the Image-Pro Plus 6.0 (Media Cybernetics, Silver Spring, MD, USA) image analysis system was used to measure the synaptic interface parameters such as synaptic cleft width, synaptic interface curvature, and postsynaptic density thickness. The synaptic interface curvature (R) was calculated based on the synaptic interface arc length (a) and the chord length (b), viz. R = a/b.

Western blot assay

The remaining rats were sacrificed by rapid decapitation and

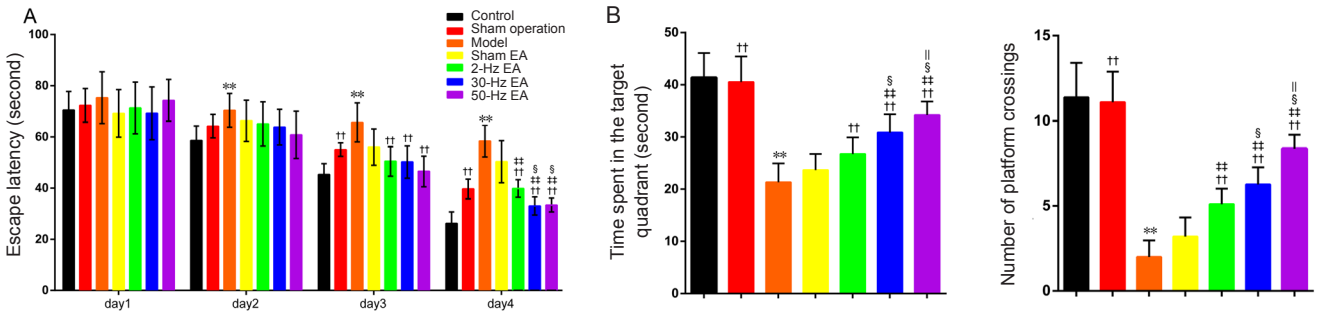

Figure 1 Effects of EA treatment on spatial learning and memory in a rat model of Alzheimer's disease (Morris water maze test).
(A) Escape latency for the place navigation trials; (B, C) time spent in the target quadrant and number of platform crossings in the spatial probe trials. Data are presented as mean ± SD (n = 12; one-way analysis of variance followed by the least significant difference test). **P < 0.01, *vs.* control group; ††P < 0.01, *vs.* model group; ‡‡P < 0.01, *vs.* sham EA group; §P < 0.05, *vs.* 2-Hz EA group; ||P < 0.05, *vs.* 30-Hz EA group. EA: Electroacupuncture.

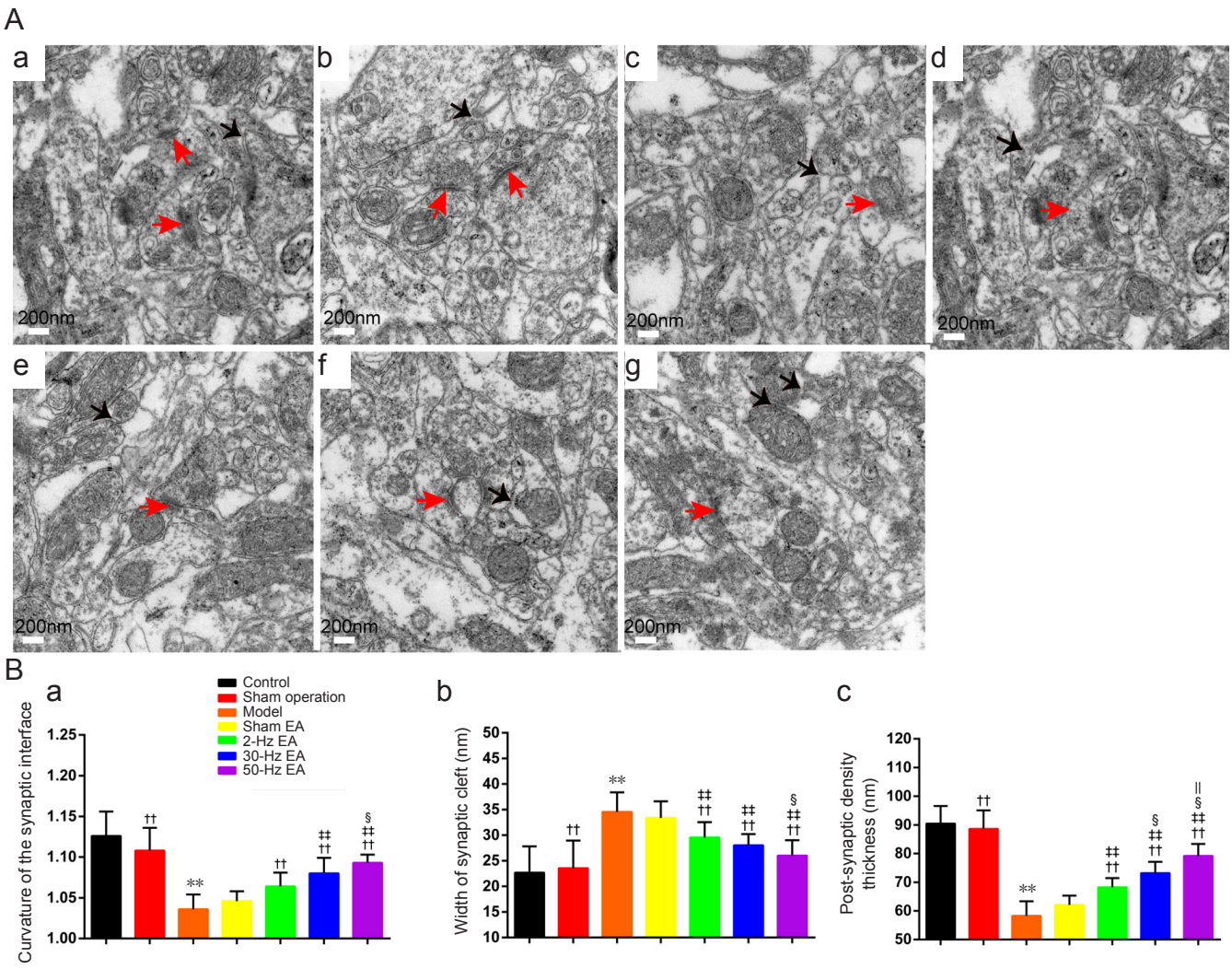

Figure 2 Effect of EA treatment on hippocampal synaptic ultrastructure in AD model rats detected by transmission electron microscopy.
(A) Effects of EA treatment on synaptic ultrastructure. EA treatment increased the synaptic curvatures, decreased the width of the synaptic cleft, and thickened the postsynaptic density; 50-Hz EA was more neuroprotective than 2-Hz or 30-Hz EA treatment. (a–g) Control group, sham operation group, model group (AD), sham EA group (AD + sham EA), 2-Hz EA group (AD + 2-Hz EA), 30-Hz EA group (AD + 30-Hz EA), and 50-Hz EA group (AD + 50-Hz EA), respectively. → : Width of synaptic cleft; →: post-synaptic density thickness. Scale bars: 200 nm. (B) Quantitative results for hippocampal synaptic ultrastructure. (a) Curvature of the synaptic interface; (b) width of synaptic cleft; (c) post-synaptic density thickness. Data are presented as the mean ± SD (n = 6; one-way analysis of variance followed by least significant difference test). **P < 0.01, *vs.* control group; ††P < 0.01, *vs.* model group; ‡‡P < 0.01, *vs.* sham-EA group; §P < 0.05, *vs.* 2-Hz EA group; ||P < 0.05, *vs.* 30-Hz EA group. EA: Electroacupuncture; AD: Alzheimer's disease.

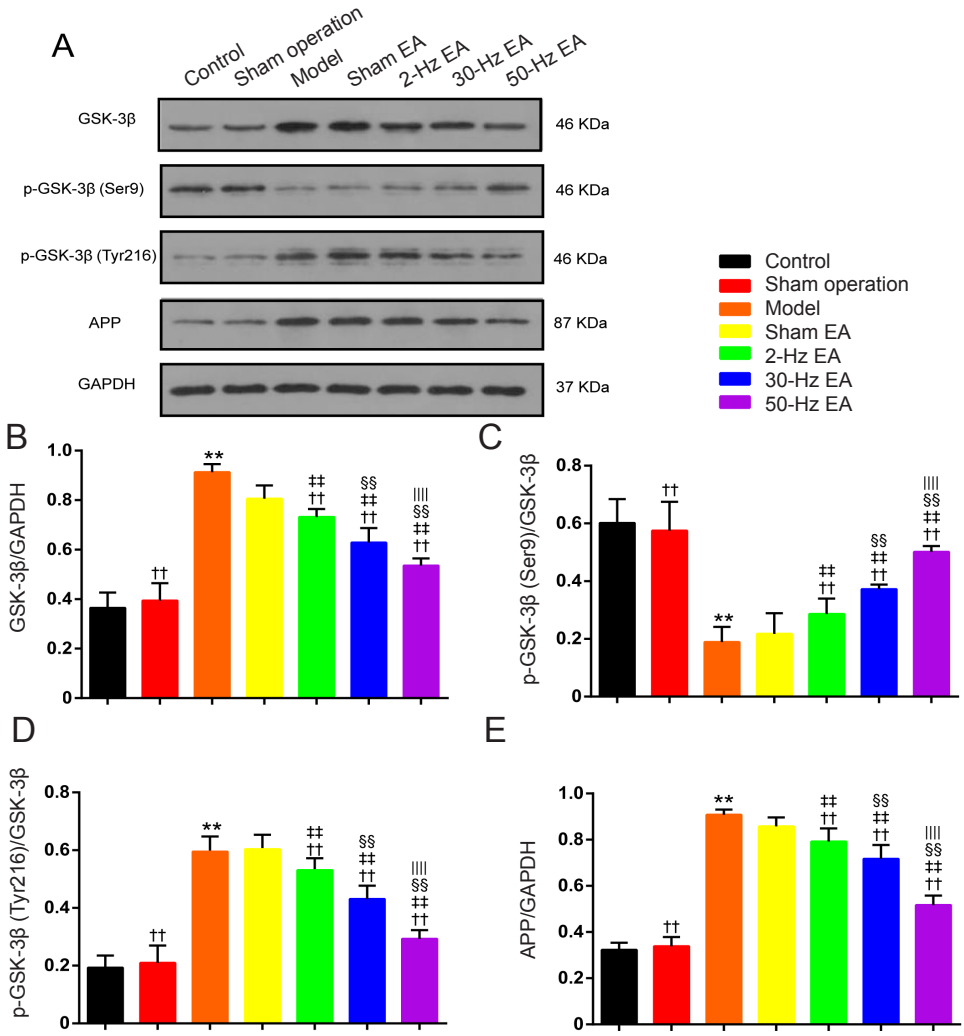

Figure 3 Effects of EA treatment on GSK-3β, p-GSK-3β (Ser9), p-GSK-3β (Tyr216), and APP protein levels in the hippocampus of Alzheimer's disease model rats.
(A) Representative western blots for GSK-3β, p-GSK-3β (Ser9), p-GSK-3β (Tyr216), and APP protein; (B–E) GSK-3β, p-GSK-3β (Ser9), p-GSK-3β (Tyr216), and APP protein expression relative to GAPDH protein. Data are presented as mean ± SD (n = 6; one-way analysis of variance followed by least significant difference test). $^{**}P < 0.01$, *vs.* control group; $^{††}P < 0.01$, *vs.* model group; $^{‡‡}P < 0.01$, *vs.* sham-EA group; $^{§§}P < 0.01$, *vs.* 2-Hz EA group; $^{||||}P < 0.01$, *vs.* 30-Hz EA group. EA: Electroacupuncture; GSK-3β: glycogen synthase kinase-3β; p-GSK-3β: phosphorylated glycogen synthase kinase-3β; APP: amyloid precursor protein; GAPDH: glyceraldehyde-3-phosphate dehydrogenase.

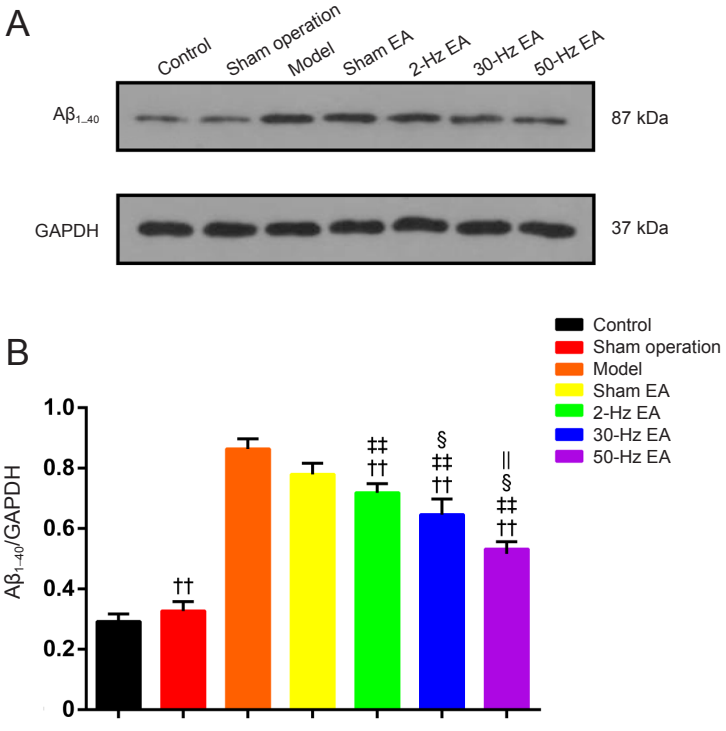

Figure 4 Effects of EA treatment on $Aβ_{1–40}$ levels in the hippocampus of Alzheimer's disease model rats.
(A) Representative western blots for $Aβ_{1–40}$; (B) $Aβ_{1–40}$ expression relative to GAPDH protein. Data are presented as mean ± SD (n = 6; one-way analysis of variance followed by least significant difference test). $^{**}P < 0.01$, *vs.* control group; $^{††}P < 0.01$, *vs.* model group; $^{‡‡}P < 0.01$, *vs.* sham-EA group; $^{§}P < 0.05$, *vs.* 2-Hz EA group; $^{||}P < 0.05$, *vs.* 30-Hz EA group. EA: Electroacupuncture; Aβ: amyloid beta; GAPDH: glyceraldehyde-3-phosphate dehydrogenase.

the hippocampus was dissected and homogenized with a glass homogenizer on ice with ice-cold radioimmunoprecipitation-assay lysis buffer containing the protease inhibitor phenylmethylsulfonylfluoride (Paxinos and Franklin, 2004). Samples containing 40 μg of protein were boiled in a sodium dodecyl sulphate mercaptoethanol sample loading buffer, separated by 10% or 12% sodium dodecyl sulfate polyacrylamide gel, and electrically transferred to a polyvinylidene fluoride membrane (Millipore, Billerica, MA, USA). Non-specific binding was blocked by incubation of the membrane in 5% skimmed milk for 1 hour. The membrane was then incubated overnight at 4°C with mouse monoclonal antibody anti-GSK3β (1:1000; Abcam, Cambridge, UK), rabbit polyclonal antibody anti-p-GSK3β (Ser9) (1:800; Abcam), rabbit polyclonal antibody anti-p-GSK3β (Tyr216) (1:800; Abcam), rabbit polyclonal antibody anti-APP (1:200; Abcam), and mouse monoclonal antibody anti-$A\beta_{1–40}$ (1:1100; Abcam). Bound primary antibody was detected with horseradish peroxidase-conjugated goat anti-rabbit IgG (1:50,000; Boster, Wuhan, China). Blots were developed using an enhanced chemiluminescence detection system (enhanced chemiluminescence kit, supplied by Thermo, Waltham, MA, USA). The optical density of the specific bands was quantified with ImageJ software (National Institutes of Health, Bethesda, MD, USA) and normalized to GAPDH.

Statistical analysis

IBM SPSS version 23.0 for Windows (IBM, Armonk, NY, USA) was used to conduct statistical analysis. All values are presented as the mean ± SD. To statistically analyze the data, one-way analyses of variance were performed, followed by post hoc comparisons using Fisher's least significant difference tests. P values < 0.05 were considered statistically significant.

Results

Effects of EA on learning and memory in AD rats

Figure 1 shows the results from the Morris water-maze tests, reflecting spatial learning and memory in the various groups of rats. In the place navigation trials (**Figure 1A**), the escape latencies for the model group were significantly higher than those for the control group starting from day 2 ($P < 0.01$). Compared with the model and sham EA groups, rats in EA treatment groups took a significantly shorter time to find the hidden platform on days 3 and 4 ($P < 0.01$). The escape latencies were significantly shorter in the 50-Hz EA and 30-Hz EA groups than in the 2-Hz EA group ($P < 0.05$), suggesting better learning and memory ability. In the spatial probe trials (**Figure 1B, C**), compared with the control group, the number of platform-location crosses and the time spent in the target quadrant were lower in the model group ($P < 0.01$). For the model rats who received EA treatment, the number of platform location crosses was frequent and the time spent in the target quadrant was longer than what was observed in untreated model rats ($P < 0.01$). These results indicated that spatial memory recall improved after the EA treatment. Moreover, the improved spatial memory recall was significantly greater in the 50-Hz EA group than in the 2-Hz or 30-Hz EA groups ($P < 0.05$).

Changes of synaptic ultrastructure in the hippocampus of AD rats after EA treatment

As shown in **Figure 2**, the analysis of hippocampal synaptic curvatures in rats after EA treatment revealed significantly higher synaptic curvatures compared with the model group ($P < 0.01$). The width of the synaptic cleft in EA-treatment groups was significantly lower than that in the model group ($P < 0.01$). The statistical analysis also revealed a significant difference between EA-treatment groups and the model group in thickness of the postsynaptic density. The postsynaptic densities in EA-treatment groups were thicker than those in the model group ($P < 0.01$). No statistically significant differences were found between the 50-Hz and the 30-Hz EA groups or between the 2-Hz and 30-Hz EA groups in synaptic curvature or width of synaptic cleft ($P > 0.05$). However, a significant difference in thickness of the postsynaptic density was observed among the three EA groups, and high-frequency EA treatment resulted in more improvement than low-frequency EA treatment ($P < 0.05$).

Effects of EA on hippocampal GSK-3β, p-GSK-3β (Ser9), p-GSK-3β (Tyr216), and APP expression in AD rats

Compared with the control and sham-operation groups, the model group exhibited significantly higher levels of GSK-3β, p-GSK-3β (Tyr216), and APP, and significantly lower amounts of p-GSK-3β (Ser9) (all $P < 0.01$). EA treatment significantly reduced total GSK-3β, p-GSK-3β (Tyr216), and APP levels and increased p-GSK-3β (Ser9) level (all $P < 0.01$ *vs.* sham EA group). We also found significant differences in protein levels between the different EA treatment groups (all $P < 0.01$ for 50-Hz EA group *vs.* 2-Hz and 30-Hz EA groups; all $P < 0.01$ for 30-Hz group *vs.* 2-Hz EA group) (**Figure 3**). Thus, the efficacy of the treatment varied systematically with stimulation frequency.

Effects of EA on hippocampal $A\beta_{1–40}$ expression in AD rats

As shown in **Figure 4**, compared with the control group, the expression of $A\beta_{1–40}$ in the hippocampus was significantly higher in the model group ($P < 0.01$). EA treatment significantly decreased the expression of $A\beta_{1–40}$ ($P < 0.01$), and the effect was frequency dependent. The 50-Hz EA treatment produced greater reduction in $A\beta_{1–40}$ than the 30-Hz or 2-Hz EA treatment ($P < 0.05$ for 50-Hz EA *vs.* 2-Hz and 30-Hz EA groups).

Discussion

This is the first study to our knowledge that has compared the effects of different EA frequencies on hippocampal synapse ultrastructure and cognitive impairment in the brains of a rat model of AD. In the present study, we found that different EA frequencies can all modify hippocampal synapse ultrastructure and improve spatial learning and memory of rats with $A\beta_{1–42}$–induced AD. Furthermore, 50-Hz EA was the most neurologically protective treatment, followed

by 30-Hz and 2-Hz EA. This was in line with our previous results (Li et al., 2016; Wang et al., 2016; Zhang et al., 2016a; Gao et al., 2017), indicating that EA treatment ameliorates cognitive deficits in rats with $A\beta_{1–42}$-induced AD.

EA frequency is an important parameter that can change the efficacy of EA treatment. Different EA frequencies can induce the release of different neurotransmitters and neuropeptides (Miao, 2016). Low-frequency EA accelerates the release of endomorphin, β-endorphin, and enkephalin, while high-frequency EA selectively increases the release of dynorphin (Han, 2004). An animal study has also shown that low-frequency EA resulted in better EA-induced cerebral ischemic tolerance than high-frequency EA (Yang et al., 2004). In the application of drug addiction, withdrawal symptoms are strongly alleviated by high-frequency EA. Low-frequency EA is better at relieving psychological dependence than high-frequency EA (Liang et al., 2002). High-frequency EA also exhibited stronger neuroprotective effects than low-frequency EA (Du and Liu, 2015).

High-frequency EA stimulation greatly improved the abnormal behavior of Parkinson's disease rats by enhancing the inhibitory effect of the cerebellar-basal ganglia-cortical loop on motor cortex (Du et al., 2011), up-regulating glial cell line-derived neurotrophic factor mRNA (Liang et al., 2003), and inhibiting the activation of microglia in the substantia nigra pars compacta (Liu et al., 2004). These data suggest that high-frequency EA may be more suitable and more effective than low-frequency EA treatment for Parkinson's disease, which is a neurodegenerative disease like AD. Combined with our previous studies, we conclude that EA treatment may ameliorate cognitive impairments in an AD mouse model. Specifically, the effect depends on EA frequency, with higher frequency EA being more effective than lower frequency EA in improving memory deficits. Further, we speculate that the selection of the best EA frequency may differ depending on the disease. Disease acupoint specificity and EA frequency might together play a critical role in determining the therapeutic effects of EA treatment. The mechanisms that underlie the EA-frequency dependent effects for the AD mouse model needs to be further investigated.

The structural parameters of the synapse are important indicators that reflect synaptic morphological plasticity and greatly affect synaptic transmission (Bourne and Harris, 2008). Synapse ultrastructure, such as synaptic curvatures, the width of the synaptic cleft, and the thickness of the postsynaptic density provide a structural basis for learning and memory abilities (Ziff, 1997; Boeckers, 2006; Bourne and Harris, 2008). In this study, synaptic ultrastructure was examined by transmission electron microscopy and appeared severely compromised in the hippocampus of the AD rat model that was established by intra-cerebroventricular injection of $A\beta_{1–42}$. In particular, we found decreased synaptic curvatures, wider synaptic clefts, and thinner postsynaptic densities compared with the control and sham operation groups, which is consistent with Chai et al. (2016). More synapses of concave or convex form, narrower widths of synaptic clefts, and thicker postsynaptic densities can enhance synaptic transmission (Ziff, 1997; Boeckers, 2006; Bourne and Harris, 2008). Additionally, compared with the model group, spatial learning and memory performance significantly increased along with rescued hippocampal synaptic structure in the EA-treated groups, which is consistent with Shao et al. (2009). The above-mentioned results suggest that EA treatment can modify synaptic structure and improve memory deficits in AD model rats. Although synaptic morphological analysis *via* transmission electron microscopy showed that some of the structural parameters of the synaptic interface were altered in the 2-Hz, 30-Hz, and 50-Hz EA groups, no statistically significant differences were observed between 2-Hz and 30-Hz EA groups or between 30-Hz and 50-Hz EA groups. We did find differences between the 2-Hz and 50-Hz EA groups, indicating that 50-Hz EA treatment for 15 days produced better neuroprotective effects than 2-Hz or 30-Hz EA treatment. In our previous study (Zhang et al., 2016a), EA treatment upregulated several synaptic protein markers, such as postsynaptic density-95 and synaptophysin, which are distributed on postsynaptic membranes and have a significant influence on axonal remodeling and regeneration, and are also involved in regulating synaptic strength (Citri and Malenka, 2008). Thus, EA treatment can dramatically rescue synaptic structural and cognitive deficits in AD mouse models.

$A\beta_{1–40}$ and $A\beta_{1–42}$ are sequential proteolytic cleavage products of APP and accumulate in the AD brain (Selkoe and Hardy, 2016). Aβ accumulation is the key factor that leads to impaired synaptic morphological plasticity and causes failure of neurotransmission (Ondrejcak et al., 2010). Therefore, we examined the expression of APP and $A\beta_{1–40}$ in the hippocampus. We found that EA treatment markedly decreased the levels of APP and $A\beta_{1–40}$, which was consistent with previous findings (Xue et al., 2009). Moreover, the effect depended on EA frequency, with 50-Hz EA resulting in the strongest protection.

Phosphorylation at the Tyr216 site activates GSK-3β, while phosphorylation at the Ser9 is inhibiting (Maqbool et al., 2016). Existing evidence supports the idea that GSK-3β upregulation can impair both morphological structure and function of synaptic plasticity, and it may underlie GSK-3β-mediated memory deficits (Zhu et al., 2007). APP itself has also been shown to be a substrate for GSK-3 *in vitro* and *in vivo* (Rockenstein et al., 2007), suggesting a role for GSK-3 in APP-transport processing and maturation (da Cruz e Silva and da Cruz e Silva, 2003). Inhibition of the GSK-3β signaling pathway by lithium in transgenic mice has been shown to produce neuroprotective effects *via* regulation of APP proteolytic processing and maturation (Rockenstein et al., 2007). Our results showed that EA treatment greatly lowered p-Tyr216- GSK-3β levels and increased p-Ser9-GSK-3β levels in the hippocampus of AD model rats. Additionally, total GSK-3β levels were also downregulated by EA treatment in an EA frequency-dependent manner, with 50-Hz EA resulting in the greatest reduction.

In addition to the preservation and modification of synapse ultrastructure, EA can also restore neural networks

(Liang et al., 2014) and stimulate neuroregeneration, which is strongly associated with synaptic function and memory (Chang et al., 2018). EA can thus influence factors involved in proliferation, which can then impact synaptic plasticity. Therefore, how EA affects factors involved in proliferation, such as neurotrophin-3 (Shimazu et al., 2006), growth-associated protein 43 (GAP-43), and brain-derived neurotrophic factor (Rosenbrock et al., 2005) needs to be investigated. In addition to regulating APP proteolytic processing and maturation, GSK-3β can also phosphorylate tau in most serine and threonine residues, which are hyperphosphorylated in paired helical filaments that impair synaptic plasticity and cognition (Llorens-Martín et al., 2014). Effects of EA on phosphorylation levels of microtubule-associated protein tau at multiple sites should also be studied.

In conclusion, EA treatment greatly improved spatial learning and memory and rescued hippocampal synaptic structure in a mouse model of AD. EA treatment inhibited GSK-3β by down-regulating phosphorylation of GSK-3β at Tyr216 and up-regulating phosphorylation of GSK-3β at Ser9, thereby leading to downregulation of APP and $A\beta_{1-40}$. Taken together, our findings strongly indicate that EA treatment can improve cognitive deficits in an EA-frequency dependent way with 50-Hz stimulation being the most protective in rat-AD models. This protective effect can be explained through the rescued hippocampal synaptic ultrastructure *via* the inhibition of GSK-3β activity, which then leads to downstream reduction in APP and Aβ. This study deepens our understanding of the mechanisms through which EA has neuroprotective effects related to AD and provides scientific experimental evidence for the optimal EA-stimulation frequency for AD in clinical application.

Author contributions: *CCY and YW wrote the paper, were responsible for the design and performance of the main experiments. LHK participated in the study design and guidance in all works and was in charge of paper authorization. FS carried out data analysis. YWW took charge of western blot assay. HZ conducted synaptic ultrastructure using electron microscopy. LT helped with the Morris water maze test. All authors approved the final version of the paper.*
Conflicts of interest: *The authors declare that there is no conflict of interests regarding the publication of this paper.*
Financial support: *This study was supported by the National Natural Science Foundation of China, No. 81373741; a grant from the Chinese Medicine and Integrated Medicine Research Projects funded by the Health and Family Planning Commission of Hubei Province of China, No. 24; a grant from the Hubei Provincial Collaborative Innovation Center of Preventive Treatment by Acupuncture and Moxibustion of China in 2014, No. 8. The funding bodies played no role in the study design, in the collection, analysis and interpretation of data, in the writing of the paper, or in the decision to submit the paper for publication.*
Institutional review board statement: *The study was approved by the Animal Ethics Committee of Hubei University of Chinese Medicine of China.*

Data sharing statement: *Datasets analyzed during the current study are available from the corresponding author on reasonable request.*
Plagiarism check: *Checked twice by iThenticate.*
Peer review: *Externally peer reviewed.*

Open peer reviewer: *Yun-Bae Kim, Chungbuk National University, Korea.*
Additional file: *Open peer review report 1.*

References

Balaraman Y, Limaye AR, Levey AI, Srinivasan S (2006) Glycogen synthase kinase 3beta and Alzheimer's disease: pathophysiological and therapeutic significance. Cell Mol Life Sci 63:1226-1235.
Beurel E, Jope RS (2006) The paradoxical pro- and anti-apoptotic actions of GSK3 in the intrinsic and extrinsic apoptosis signaling pathways. Prog Neurobiol 79:173-189.
Boeckers TM (2006) The postsynaptic density. Cell Tissue Res 326:409-422.
Bourne JN, Harris KM (2008) Balancing structure and function at hippocampal dendritic spines. Annu Rev Neurosci 31:47-67.
Bromley-Brits K, Deng Y, Song W (2011) Morris water maze test for learning and memory deficits in Alzheimer's disease model mice. J Vis Exp:2920.
Brugg B, Matus A (1991) Phosphorylation determines the binding of microtubule-associated protein 2 (MAP2) to microtubules in living cells. J Cell Biol 114:735-743.
Chai JX, Li HH, Wang YY, Chai Q, He WX, Zhou YM, Hu XD, Wang ZH (2016) Effect of diallyl disulfide on learning and memory abilities and hippocampal synapses in mouse models of Alzheimer's disease. Nan Fang Yi Ke Da Xue Xue Bao 36:1417-1422.
Chang QY, Lin YW, Hsieh CL (2018) Acupuncture and neuroregeneration in ischemic stroke. Neural Regen Res 13:573-583.
Cheng LL, Ding MX, Xiong C, Zhou MY, Qiu ZY, Wang Q (2012) Effects of electroacupuncture of different frequencies on the release profile of endogenous opioid peptides in the central nerve system of goats. Evid Based Complement Alternat Med 2012:476457.
Citri A, Malenka RC (2008) Synaptic plasticity: multiple forms, functions, and mechanisms. Neuropsychopharmacology 33:18-41.
da Cruz e Silva EF, da Cruz e Silva OA (2003) Protein phosphorylation and APP metabolism. Neurochem Res 28:1553-1561.
Du F, Liu S (2015) Electroacupuncture with high frequency at acupoint ST-36 induces regeneration of lost enteric neurons in diabetic rats via GDNF and PI3K/AKT signal pathway. Am J Physiol Regul Integr Comp Physiol 309:R109-118.
Du J, Sun ZL, Jia J, Wang X, Wang XM (2011) High-frequency electro-acupuncture stimulation modulates intracerebral gamma-aminobutyric acid content in rat model of Parkinson's disease. Sheng Li Xue Bao 63:305-310.
Folch J, Petrov D, Ettcheto M, Abad S, Sánchez-López E, García ML, Olloquequi J, Beas-Zarate C, Auladell C, Camins A (2016) Current research therapeutic strategies for Alzheimer's disease treatment. Neural Plast 2016:8501693.
Gao S, Kong LH, Yu CC, Yao GJ (2017) Mechanism of different frequencies of electroacupuncture in treating neuropathy in rats with Alzheimer's disease. Zhongguo Quanke Yixue 20:1449-1456.
Guo Y, Kong LH (2016) Guidelines on Experiment Design of Experimental Acupuncture Science. Beijing: China Press of Traditional Chinese Medicine.
Han JS (2004) Acupuncture and endorphins. Neurosci Lett 361:258-261.
Hane FT, Lee BY, Leonenko Z (2017) Recent progress in Alzheimer's disease research, Part 1: Pathology. J Alzheimers Dis 57:1-28.
Hernández F, Borrell J, Guaza C, Avila J, Lucas JJ (2002) Spatial learning deficit in transgenic mice that conditionally over-express GSK-3beta in the brain but do not form tau filaments. J Neurochem 83:1529-1533.
Itarat W, Jones DG (1993) Morphological characteristics of perforated synapses in the latter stages of synaptogenesis in rat neocortex: stereological and three-dimensional approaches. J Neurocytol 22:753-764.
Kimura K, Ryujin T, Uno M, Wakayama I (2015) The effect of electroacupuncture with different frequencies on muscle oxygenation in humans. Evid Based Complement Alternat Med 2015:620785.

Kocahan S, Dogan Z (2017) Mechanisms of Alzheimer's disease pathogenesis and prevention: the brain, neural pathology, n-methyl-d-aspartate receptors, Tau protein and other risk factors. Clin Psychopharmacol Neurosci 15:1-8.

Law BYK, Wu AG, Wang MJ, Zhu YZ (2017) Chinese medicine: a hope for neurodegenerative diseases? J Alzheimers Dis 60:S151-S160.

Li W, Kong LH, Wang H, Shen F, Wang YW, Zhou H, Sun GJ (2016) High-frequency electroacupuncture evidently reinforces hippocampal synaptic transmission in Alzheimer's disease rats. Neural Regen Res 11:801-806.

Liang MH, Chuang DM (2007) Regulation and function of glycogen synthase kinase-3 isoforms in neuronal survival. J Biol Chem 282:3904-3917.

Liang P, Wang Z, Qian T, Li K (2014) Acupuncture stimulation of Taichong (Liv3) and Hegu (LI4) modulates the default mode network activity in Alzheimer's disease. Am J Alzheimers Dis Other Demen 29:739-748.

Liang XB, Liu XY, Li FQ, Luo Y, Lu J, Zhang WM, Wang XM, Han JS (2002) Long-term high-frequency electro-acupuncture stimulation prevents neuronal degeneration and up-regulates BDNF mRNA in the substantia nigra and ventral tegmental area following medial forebrain bundle axotomy. Brain Res Mol Brain Res 108:51-59.

Liang XB, Luo Y, Liu XY, Lu J, Li FQ, Wang Q, Wang XM, Han JS (2003) Electro-acupuncture improves behavior and upregulates GDNF mRNA in MFB transected rats. Neuroreport 14:1177-1181.

Lin SY, Gao J, Yin ZL, Zhou LJ, Chen X (2013) Impacts of the different frequencies of electroacupunctrue on cognitive function in patients after abdominal operation under compound anesthesia of acupuncture and drugs. Zhongguo Zhen Jiu 33:1109-1112.

Liu XY, Zhou HF, Pan YL, Liang XB, Niu DB, Xue B, Li FQ, He QH, Wang XH, Wang XM (2004) Electro-acupuncture stimulation protects dopaminergic neurons from inflammation-mediated damage in medial forebrain bundle-transected rats. Exp Neurol 189:189-196.

Llorens-Martín M, Jurado J, Hernández F, Avila J (2014) GSK-3beta, a pivotal kinase in Alzheimer disease. Front Mol Neurosci 7:46.

Lovestone S, Boada M, Dubois B, Hüll M, Rinne JO, Huppertz HJ, Calero M, Andres MV, Gómez-Carrillo B, León T, del Ser T, ARGO investigators (2015) A phase II trial of tideglusib in Alzheimer's disease. J Alzheimers Dis 45:75-88.

Maqbool M, Mobashir M, Hoda N (2016) Pivotal role of glycogen synthase kinase-3: A therapeutic target for Alzheimer's disease. Eur J Med Chem 107:63-81.

Miao L (2016) Electroacupuncture promotes the proliferation and differentiation of neural stem cells in the rat hippocampus of spleen deficiency syndrome. Zhongguo Zuzhi Gongcheng Yanjiu 20:4859-4864.

Muresan Z, Muresan V (2005) Coordinated transport of phosphorylated amyloid-beta precursor protein and c-Jun NH2-terminal kinase-interacting protein-1. J Cell Biol 171:615-625.

O'Hare E, Weldon DT, Mantyh PW, Ghilardi JR, Finke MP, Kuskowski MA, Maggio JE, Shephard RA, Cleary J (1999) Delayed behavioral effects following intrahippocampal injection of aggregated A beta (1-42). Brain Res 815:1-10.

Ondrejcak T, Klyubin I, Hu NW, Barry AE, Cullen WK, Rowan MJ (2010) Alzheimer's disease amyloid beta-protein and synaptic function. Neuromolecular Med 12:13-26.

Paxinos G, Franklin KB (2004) The Mouse Brain in Stereotaxic Coordinates. San Diego, CA, USA: Gulf Professional Publishing.

Peng XW, Dong KL (2009) Clinical observation on acupuncture combined with Yizhi Jiannao granules for treatment of Alzheimer's disease. Zhongguo Zhen Jiu 29:269-271.

Prince M, Bryce R, Albanese E, Wimo A, Ribeiro W, Ferri CP (2013) The global prevalence of dementia: a systematic review and meta-analysis. Alzheimers Dement 9:63-75.e2.

Rockenstein E, Torrance M, Adame A, Mante M, Bar-on P, Rose JB, Crews L, Masliah E (2007) Neuroprotective effects of regulators of the glycogen synthase kinase-3beta signaling pathway in a transgenic model of Alzheimer's disease are associated with reduced amyloid precursor protein phosphorylation. J Neurosci 27:1981-1991.

Rosenbrock H, Koros E, Bloching A, Podhorna J, Borsini F (2005) Effect of chronic intermittent restraint stress on hippocampal expression of marker proteins for synaptic plasticity and progenitor cell proliferation in rats. Brain Res 1040:55-63.

Selkoe DJ (2002) Alzheimer's disease is a synaptic failure. Science 298:789-791.

Selkoe DJ, Hardy J (2016) The amyloid hypothesis of Alzheimer's disease at 25 years. EMBO Mol Med 8:595-608.

Shao X, Yu SG, Lu SF, Tang Y, Yin HY (2009) Influence of electro-acupuncture therapy on synaptic ultrastructure of hippocampal neuron of SAMP8 rats. ZHongguo Laonian Xue Zazhi 29:780-782.

Shimazu K, Zhao M, Sakata K, Akbarian S, Bates B, Jaenisch R, Lu B (2006) NT-3 facilitates hippocampal plasticity and learning and memory by regulating neurogenesis. Learn Mem 13:307-315.

Wang K, Zhang R, He F, Lin LB, Xiang XH, Ping XJ, Han JS, Zhao GP, Zhang QH, Cui CL (2012) Electroacupuncture frequency-related transcriptional response in rat arcuate nucleus revealed region-distinctive changes in response to low- and high-frequency electroacupuncture. J Neurosci Res 90:1464-1473.

Wang Y, Li W, Zhang KK, Wang H, Kong LH (2016) Effect of electroacupuncture with different frequencies on learning and memory ability and synapse in hippo-camp in rats with Alzheimer's disease. Zhongguo Kangfu Lilun yu Shijian 22:635-639.

Xue WG, Zhang Z, Bai LM, Xu H, Wu HX (2009) Effect of electroacupuncture on the behavior and the expression of amyloid beta-protein, amyloid precursor protein and ChAT in APP 695 V 717 I transgenic mice. Zhen Ci Yan Jiu 34:152-158.

Yang J, Xiong LZ, Wang Q, Liu YH, Chen SY, Xu N (2004) Effects of Different stimulating parameters and their various combinations on electroacupuncture-induced cerebral ischemic tolerance in rats. Zhongguo Zhen Jiu 24:208-212.

Zhang KK, Kong LH, Wang Y, Yao GJ, Yu CC, Gao S, Shen F, Meng PY, Wang YW (2016a) Effects of electro-acupuncture of different frequency on the SYN protein and PSD-95 protein expression of rats with Alzheimer's disease. Shizhen Guoyi Guoyao 27:2539-2542.

Zhang Y, Huang LJ, Shi S, Xu SF, Wang XL, Peng Y (2016b) L-3-n-butylphthalide rescues hippocampal synaptic failure and attenuates neuropathology in aged APP/PS1 mouse model of Alzheimer's disease. CNS Neurosci Ther 22:979-987.

Zhou J, Peng W, Xu M, Li W, Liu Z (2015) The effectiveness and safety of acupuncture for patients with Alzheimer disease: a systematic review and meta-analysis of randomized controlled trials. Medicine (Baltimore) 94:e933.

Zhu D, Bai L, Zhang X, Xu X, Zhang J (2015) Research progress on quantification of electroacupuncture parameters. Zhongguo Zhen Jiu 35:525-528.

Zhu H, Dong KL, Wu Y, Zhang T, Li RM, Dai SS, Wang HL (2010) Influence of acupuncture on isoprostane in patients with Alzheimer's disease. Zhongguo Zhen Jiu 30:18-21.

Zhu LQ, Wang SH, Liu D, Yin YY, Tian Q, Wang XC, Wang Q, Chen JG, Wang JZ (2007) Activation of glycogen synthase kinase-3 inhibits long-term potentiation with synapse-associated impairments. J Neurosci 27:12211-12220.

Ziff EB (1997) Enlightening the postsynaptic density. Neuron 19:1163-1174.

(*Copyedited by Yu J, Li CH, Qiu Y, Song LP, Zhao M*)